Noise-Mediated Cooperative Behavior and Signal Detection in dc SQUIDs

Mario E. Inchiosa* and Adi R. Bulsara†

Space and Naval Warfare Systems Center, San Diego
Code D-364, San Diego, CA 92152-5001

Abstract. We study the detection of very weak time-periodic magnetic signals via a double-junction (dc) Superconducting Quantum Interference Device (SQUID). The device, represented by two coupled nonlinear differential equations for the quantum mechanical junction phases, admits of long-time static or oscillatory solutions, the transition being controllable by experimental parameters. Signal detection is optimal when the device is "tuned" to the onset of the oscillatory solutions; i.e., when the minima in the 2D potential function disappear. Modeling the device via a derived input-output transfer characteristic yields a response (quantified via the signal-to-noise ratio at the signal frequency) in good agreement with recent experiments. We also present some preliminary results pertaining to coupled dc SQUIDs, taking into account the (incoherent) thermal noise sources in each of the Josephson junctions. As might be expected from previous work, coupling the SQUIDs and/or summing their outputs enhances the response to the external signal.

I INTRODUCTION

Superconducting Quantum Interference Devices (SQUIDs) [1] are the most sensitive detectors of magnetic fields; however, they are quite vulnerable to environmental noise, thermal noise in the junctions, or noise coupled in from the biasing and readout electronics. Operated in the conventional flux-locked mode wherein the device is kept "locked" to an operating point in the linear regime of its transfer characteristic via feedback electronics, a very small amount of noise is often sufficient to lose the operating point...the so-called "slew-rate" problem. Allowing the SQUID to operate as a free-running nonlinear dynamic device can enhance the dynamic range if nonlinear phenomena are carefully utilized to alleviate noise problems. The objective in this case is not necessarily an enhancement of the SQUID response's SNR, rather it could be an effective lowering of the noise floor of the readout system, resulting in an increase in the entire system's SNR, signal detection probability, and dynamic range.

Recent experiments and calculations have explored the basic Stochastic Resonance (SR) effect, and some variations, in a single-junction (rf) SQUID [3,4]. This

device consists of a single Josephson junction shorted by a superconducting loop, and coupled to the target signal via cooled pickup coils. The dynamics are in general multistable, with the magnetic flux through the superconducting loop being quantized in units of the flux quantum $\Phi_0 \equiv h/2e$. In the presence of the junction, the magnetic flux Φ through the loop, in response to an applied time-dependent magnetic flux Φ_e, evolves according to the dynamics [1],

$$\tau_L \dot{x} = -U'(x). \tag{1}$$

[Note that in this paper the letter x (possibly subscripted) represents a magnetic flux normalized to the flux quantum; e.g., $x \equiv \Phi/\Phi_0$.] In (1), x represents the (normalized) magnetic flux through the loop, the dot denotes time-differentiation, and the potential function $U(x) = \frac{1}{2}(x - x_e)^2 - \frac{\beta_s}{4\pi^2}\cos 2\pi x$ is multistable when $\beta_s > \beta_{sc}$ (and monostable otherwise); $\beta_{sc} = 1$ for $x_e = 0$. $x_e = x_i + x_0$ is the externally applied flux, x_0 is a dc magnetic flux, and $x_i = \eta(t) + y(t)$ is an ac magnetic flux consisting of a deterministic component $\eta(t)$ and a background, non-thermal noise $y(t)$ (fed in from the bias or readout electronics or the environment). The noise is usually modeled as Gaussian and exponentially correlated, with correlation time much less that the SQUID time constant τ_L, which is typically the smallest time-scale of the problem (here we are assuming the SQUID's thermal noise to be negligible). The inertial (capacitative) term in the dynamics is absent because in most applications one incorporates a shunt resistance across the junction [1]; this removes hysteresis in its voltage-current characteristic.

The signal detection properties of the rf SQUID have been extensively analyzed for the case of a multistable potential function. In the presence of a known time-periodic bias signal, an unknown dc "target" magnetic flux x_0 renders the potential asymmetric, and all harmonics of the (known) sinusoidal bias flux $\eta(t)$ appear. An SR effect occurs at every harmonic and the spectral amplitudes are dependent on the magnitude of the target dc signal. For a potential whose minima all come in symmetric pairs (e.g. a symmetric double-well potential), only the odd multiples of the signal frequency appear in the power spectral density (PSD) of the motion. Hence, the appearance of the even multiples of the bias signal, together with the change in their spectral amplitudes can be used as a means to detect and quantify the target signal [4]. In complex operating scenarios, if a "clean" window is known to exist in a particular regime of the frequency spectrum, we can choose the frequency of $\eta(t)$ to carry out our detection in that window. This technique makes no attempt to eliminate low frequency noise or to enhance the output SNR in the conventional sense; it merely shifts the detection to a more acceptable part of the frequency spectrum. This idea affords a novel technique that can be applied to SQUIDs (particularly high temperature SQUIDs) as well as other nonlinear dynamic sensors that are noise-constrained at certain frequencies.

In the monostable regime, it is convenient to characterize the SQUID [6] as a memoryless static nonlinearity, a *non*-dynamical system characterized only via an input-output transfer characteristic (TC). This characteristic is found by setting

the left hand side of (1) to zero, solving the resultant transcendental equation for $x(t)$ and plotting the "shielding flux" $x_s(t) \equiv x(t) - x_e(t)$ vs. the input flux $x_i(t)$. Having obtained the TC, one can analytically apply the sinusoidal input signal plus Gaussian noise to it, and compute the autocorrelation function $\langle x_s(t)x_s(t+h)\rangle$ and its associated power spectral density [6], whence we compute the SNR at the fundamental of the applied signal. On a 3D plot of SNR vs. dc bias x_0 and nonlinearity β_s, one observes distinct regimes of SNR crests and troughs. This form of SNR maximization differs from SR insofar as one obtains the optimal response by tuning control parameters (in this case, the dc bias flux and the nonlinearity parameter), rather than the input noise strength. The theoretical results are well supported by experiments, and the response of such static nonlinearities to more general (e.g. wideband) signals has also been investigated in a recent publication [7] using information-theoretic distance measures to characterize the output.

With this preamble, we now turn to our recent work on the two-junction or dc SQUID [8,9]. Unlike the rf SQUID described above, the dc SQUID is characterized by a 2D potential function and can exhibit spontaneous oscillatory solutions under the appropriate system preparation. We first describe the single dc SQUID, and then outline some ongoing research on the response of two flux-coupled dc SQUIDs.

II NONLINEAR AMPLIFICATION IN A DC SQUID

The dc SQUID consists of two Josephson junctions inserted into a superconducting loop [1]; we assume, for convenience, that the insertion is symmetric. Conventionally, the voltage measured across the Josephson junctions is taken as the SQUIDs "output." Instead, we take the circulating current I_s (experimentally measured via the associated "shielding flux") as output. This setup was developed for studying SR in dc SQUIDs operating in a hysteretic regime. However, much higher output signal strengths and SNRs were discovered by using dc bias currents large enough to take the device beyond the hysteretic regime into the regime of oscillatory solutions. These higher input-output gains result from the rapid change of I_s with Φ_e close to where the dynamics change from static to oscillatory.

In the presence of an external magnetic flux Φ_e, one obtains [1] a loop flux consisting of the (geometrical) component Φ_e together with a contribution arising from the induced circulating or shielding current I_s that tends to screen the applied flux:

$$\Phi = \Phi_e + LI_s, \tag{2}$$

L being the loop inductance. The Josephson currents in each arm of the "interferometer" are $I_0 \sin\delta_1$ and $I_0 \sin\delta_2$, with the junctions assumed to be identical with critical currents I_0, and with $\delta_{1,2}$ being the quantum phases. The wave-function must remain single-valued around the SQUID loop, leading to the phase continuity condition,

$$\delta_2 - \delta_1 = 2\pi n - 2\pi\Phi/\Phi_0, \tag{3}$$

n being an integer, and $\Phi_0 \equiv h/2e$ the flux quantum. Combining (2) and (3) and setting $n = 0$, we find for the circulating current I_s,

$$\beta\frac{I_s}{I_0} = \delta_1 - \delta_2 - 2\pi\frac{\Phi_e}{\Phi_0}, \tag{4}$$

where $\beta \equiv 2\pi LI_0/\Phi_0$ is the nonlinearity parameter. In the absence of noise and the target magnetic flux (taken to be sinusoidal in this work), we can use the RSJ model to write down equations for the currents in the two arms of the SQUID via a lumped circuit representation [1]; expressed via the Josephson relations $\dot{\delta}_i = 2eV_i/\hbar$ linking the voltage and the quantum phase difference across the junction i, these equations take the form,

$$\tau\dot{\delta}_1 = \frac{I_b}{2} - I_s - I_0\sin\delta_1, \quad \tau\dot{\delta}_2 = \frac{I_b}{2} + I_s - I_0\sin\delta_2, \tag{5}$$

where $\tau \equiv \hbar Re/2$, R being the normal state resistance of the junctions. The dc bias current I_b is applied symmetrically to the loop. In experiments [8], the bias current and applied flux are externally controllable. This is a critical point, since, as will become evident below, it permits us to manipulate the shape of the 2D potential function that characterizes the SQUID dynamics and thereby the input-output TC that governs the response (note that the solutions of (5) can be oscillatory, even in the absence of external inputs). Rescaling the time by τ/I_0, one can write the above in the form $\dot{\delta}_i = -\frac{\partial U}{\partial\delta_i}$ with the 2D potential function defined as

$$U(\delta_1,\delta_2) = -\cos\delta_1 - \cos\delta_2 - J(\delta_1+\delta_2) + (2\beta)^{-1}(\delta_1 - \delta_2 - 2\pi\Phi_{ex})^2, \tag{6}$$

where we introduce the dimensionless bias current $J \equiv I_b/(2I_0)$ and normalized applied flux $\Phi_{ex} \equiv \Phi_e/\Phi_0$, taken to be solely dc for the moment.

The SQUID's Josephson junctions are always in a superconducting state when the potential (6) has stable minima; it is readily apparent that the symmetry of the potential and the depth of the minima are controlled by the adjustable parameters J and Φ_{ex}. This configuration (including the problem of thermal activation out of the stable states of the potential) has been discussed in the literature [10]. After a brief transient, the phase angles $\delta_{1,2}$ achieve constant steady-state values and one obtains the conditions for the minima via $\dot{\delta}_{1,2} = 0$. This leads to the current equations

$$I_b = I_0(\sin\delta_1 + \sin\delta_2), \quad 2I_s = I_0(\sin\delta_2 - \sin\delta_1). \tag{7}$$

Of course, these equations may also be written down by applying Kirchoff's laws directly to the lumped circuit representation of the SQUID. Using the phase continuity relation, we are finally able to write down a transcendental equation for the circulating current I_s:

$$\frac{I_s}{I_0} = -\sin\left(\pi\Phi_{ex} + \frac{\beta I_s}{2I_0}\right)\cos\left[\sin^{-1}\left(J + \frac{I_s}{I_0}\right) + \pi\Phi_{ex} + \frac{\beta I_s}{2I_0}\right]. \tag{8}$$

Equation (8) may be solved numerically for the circulating current; the ensuing TC is periodic in the applied flux Φ_{ex} and possibly hysteretic, with the hysteresis loop width controlled by the bias current J. For $J = 0$ one obtains hysteresis for any nonlinearity β; for $0 < J \leq 1$, hysteresis occurs over some range of β. It is most important to note that equations (7) and, therefore, (8) are valid only when the potential has stable minima. In this regime, the externally applied bias current is matched by the sum of the junction supercurrents. When this balance is exceeded, a finite voltage V (corresponding to a normal loop current V/R) appears across the device. The maximum applied current (before the device enters its "voltage state") is clearly $2I_0$ in the absence of an applied external flux. However, in the presence of the external flux, one must compute the the critical applied current at which the voltage state appears. In this regime, one obtains oscillatory solutions for the phases δ_i (modulo 2π) and the circulating current I_s, reminiscent of self-excited or relaxation oscillators that are encountered in systems with negative damping [11]. For the system at hand, this behavior may be traced to the description in terms of the two coupled first-order differential equations (5), together with a non-zero applied current J. In fact, it may be shown that, *only* in the superconducting regime (where the potential has stable minima), the SQUID dynamics (5) may be reduced to the 1D form, in terms of the normalized flux variable x:

$$\tau_s \dot{x} = -x - x_e - \frac{\beta}{2\pi}\sin\pi x \cos Z, \tag{9}$$

where we set $\tau_s = \frac{\beta\tau}{2I_0}$ and $Z = \pi x + \arcsin\left[J + \frac{2\pi}{\beta}(x - x_e)\right]$. Equating the right hand side of (9) to zero and solving (numerically) for the x vs. x_e TC yields a curve identical to that obtained from the transcendental form (8), after we express I_s in terms of x. Note that, in this regime, the potential (6) can readily be transformed into a single-variable potential $U(x)$, whose gradient yields (up to a multiplicative constant) the negative of the right hand side of (9); this, of course, is to be expected.

We are interested, primarily, in operating the SQUID in the regime that yields the optimal response to a target input signal; further, we would like to (as outlined in the preceding section) obtain this response only by adjusting the system parameters, without having to alter the input SNR. From a computational standpoint, it is certainly more convenient to work in the non-hysteretic regime wherein the output variable (in this case, the circulating current I_s) is single-valued in the input. Then, one simply constructs the TC and applies the signal and noise to the input, as has been done in our earlier work [6]. In the hysteretic regime, on the other hand, one must integrate the coupled equations (5) and compute power spectra by averaging time series; this can prove cumbersome in some cases, and is certainly dependent on computing power. For the rf SQUID, outlined in the preceding section, hysteresis is removed by decreasing the nonlinearity parameter below a critical value. In the

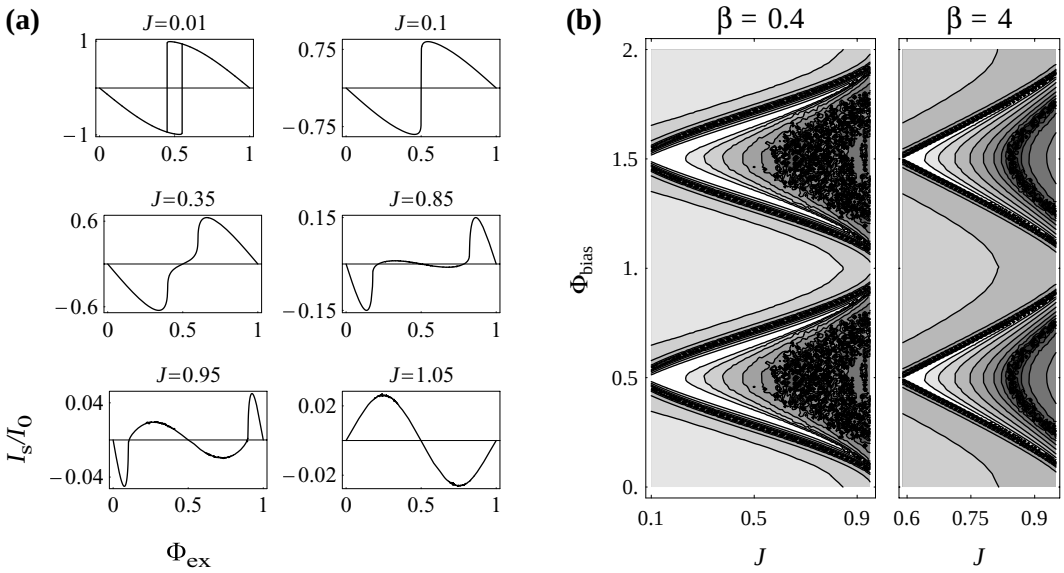

FIGURE 1. (a) Transfer characteristic: time-averaged circulating current (see text) I_s/I_0 vs. applied flux Φ_{ex} for $\beta = 0.4$. (b) Contour plot showing theoretically predicted output SNR (taken at target signal frequency), in the oscillatory solutions regime, vs. bias parameters $\Phi_{\rm bias}$ and J. SNR scale (black-to-white) corresponds to -28 dB to 32 dB, with contour lines spaced 5 dB apart (SNR values of -28 dB or less are represented by black; a "speckled" appearance in the black regions of the $\beta = 0.4$ plot is due to limited numerical precision).

current situation, however, one may obtain hysteresis for any β, with the applied current J controlling the regime of hysteresis. In experiments and simulations, one obtains the best response when the TC is non-hysteretic; this might be expected since, in general, the optimal response occurs in the linear or quasi-linear regime. The bulk of our work is, therefore, carried out in the non-hysteretic regime, with $\beta \approx 1$ used in most of our simulations. In this regime, for a range of applied fluxes around $\Phi_{ex} = 0.5$ the SQUID admits of oscillatory solutions and the potential ceases to have minima, with the conservation relations (7) violated.

We now examine the dc SQUID in the regime of oscillatory solutions in some greater detail. These solutions arise when the bias current J is increased to the point where the first of the conservation relations (7) cannot hold without the presence of an additional (normal) current term. Let Φ_{ex1} be the critical flux at which, as Φ_{ex} is increased from 0 to 1/2, the potential's minima disappear and oscillatory solutions replace static ones. For Φ_{ex} increasing from 1/2 to 1, the oscillatory solutions disappear at $\Phi_{ex2} \equiv 1 - \Phi_{ex1}$. Recent calculations [9] predict the critical external dc flux Φ_{ex1}, for a given bias current J. The oscillation period tends to infinity very close to Φ_{ex1}, decreases as $\Phi_{ex} \to 1/2$, and increases again as $\Phi_{ex} \to \Phi_{ex2}$. The interval (Φ_{ex1}, Φ_{ex2}) of the oscillatory solutions increases with J.

Other researchers [12] have investigated the oscillatory regime via a computation

of the voltage across the Josephson junctions; the Josephson relations relate this voltage (which can be experimentally measured) to the frequency of the oscillations. Here, however, we consider the screening current I_s as the variable of interest. Our experiments [8] are able to measure the current, with one important caveat: due to the extremely high oscillation frequency [predicated by the constant τ in (5)], the experiments actually measure the time-averaged current I_s. The TC is then simply a plot of this I_s vs. the applied flux Φ_{ex}. An analytic computation of I_s has not yet been accomplished; however, one may numerically solve the dynamics (5), compute the (oscillating) I_s and then compute the time-average. A family of TCs obtained in this manner is shown in Fig. 1(a).

From the TCs, we can calculate the output SNR in response to an applied flux consisting of a time-sinusoidal signal, colored noise, and a dc component $\Phi_{\rm bias}$ (normalized to Φ_0). The input signal power $S_{\rm in}$ and noise power $N_{\rm in}$ are taken arbitrarily small so that they are transformed in a nearly linear manner by the device, simply being multiplied by the slope or gain G of the TC at the bias value $\Phi_{\rm bias}$. Note that the strongly nonlinear response regime has been studied in [6]. We assume that the signal and noise lie well within the SQUID bandwidth τ_L^{-1}. In the experiment a second SQUID, operating as a conventional (flux-locked) device, reads the output of the "sensing" SQUID; hence it introduces a noise floor N_f (taken equal to $N_{\rm in}$) into the measurement of the sensing SQUID. Taking into account the power coupling efficiency ϵ between the SQUIDs, we may write down for the output SNR,

$$R = \frac{S_{\rm in} G^2 \epsilon}{N_{\rm in} G^2 \epsilon + N_f} = \frac{R_{\rm in} G^2 \epsilon}{G^2 \epsilon + 1}. \tag{10}$$

In Fig. 1(b) we show the output SNR vs. the control parameters J and $\Phi_{\rm bias}$. The $\Phi_{\rm bias}$ values shown cover two periods of the TC, and the SNR contour plots reflect this periodicity. The J values shown cover the range over which the dc SQUID has both static and oscillatory states (depending on the value of $\Phi_{\rm bias}$). This range is characterized by a split in the maximal SNR; one observes "bifurcating crests" separated, vertically, by $\Phi_{ex2} - \Phi_{ex1}$. The SNR depends on the slope of the TC, being maximal on the segments with maximum slope. The troughs running just outside the crests correspond to zero-slope points at minima and maxima of the TC. With increasing β, the range of J values yielding both static and oscillatory solutions shrinks. Also, for large β's the crests become less evident, but the troughs remain. For $J > 1$, the Josephson junctions are normal and the transfer characteristic has a much reduced range, resulting in a minimal output SNR.

The theoretical predictions have been shown [9] to be in very good agreement with experimental results [8]. It is particularly gratifying to be able to "tune" the response (i.e. adjust the TC) to the optimal, by adjusting the experimentally accessible parameters J and $\Phi_{\rm bias}$, since the nonlinearity β cannot easily be adjusted after fabrication. The agreement with experimental results could be substantively improved by a systematic consideration of coupling effects between the sensing

and readout SQUIDs. It is also important to study coupling effects as a potential means of reducing the effective noise floor of the readout; our earlier work [13] on coupled systems indicates that substantial enhancements of the output SNR should accrue, with carefully applied coupling. In the following section, we outline some preliminary results for coupled dc SQUIDs.

III COUPLED DC SQUIDS

Motivated by the plethora of recent results [13] showing that coupling and noise can, cooperatively, enhance the response in nonlinear dynamic devices, we consider and present some preliminary results involving coupled dc SQUIDs. In general, the coupling can be global or local, linear or nonlinear. Here we consider n SQUIDs with global linear coupling. The k^{th} SQUID ($k = 1, \ldots, n$) is described by the (coupled) dynamics of the phase angles δ_{kj} ($j = 1, 2$):

$$\frac{\tau_k}{I_{0k}}\dot{\delta}_{kj} = J_k + (-1)^j \frac{I_k}{I_{0k}} - \sin\delta_{kj}, \tag{11}$$

where I_k represents the circulating current (we have dropped the subscript s for convenience), and $J_k = I_{ek}/(2I_{0k})$ the (normalized) externally applied bias current; I_{0k} is the critical current of the junctions, and $\tau_k \equiv \hbar R_k e/2$, with R_k being the normal state resistance of the junctions (we assume that each SQUID is comprised of two identical junctions, with the differences in β's arising via different loop inductances L_k). The circulating current is inductively coupled (we assume equal mutual inductance coupling of strength M) to the loop currents in the remaining SQUIDs:

$$\beta_k \frac{I_k}{I_{0k}} = \delta_{k1} - \delta_{k2} - \frac{2\pi}{\Phi_0}\left(\Phi_{ek0} + M\sum_{m\neq k} I_m\right), \tag{12}$$

where Φ_{ek0} is the external flux at the k^{th} SQUID. Noting that the bias currents I_m appearing on the right hand side of (12) are, in turn, coupled to every other bias current (including I_k), we see that we will get an infinite nested series on the right hand side of (12) and, hence, in (11). For the purposes of this paper, we consider some simplified situations, namely a pair of (possibly non-identical) SQUIDs and n identical SQUIDs.

First we consider the scenario of two inductively coupled dc SQUIDs (for this case global and local coupling are of course equivalent). The circulating currents in the two loops evolve via dynamics analogous to (4):

$$\beta_1 \frac{I_1}{I_{01}} = \delta_{11} - \delta_{12} - \frac{2\pi\Phi_{e1}}{\Phi_0}, \quad \beta_2 \frac{I_2}{I_{02}} = \delta_{21} - \delta_{22} - \frac{2\pi\Phi_{e2}}{\Phi_0}. \tag{13}$$

From (11), we may write down equations for the coupled phase angles for the SQUIDs, after some manipulation:

$$\frac{\tau_1}{I_{01}}\dot{\delta}_{11} = J_1 - \frac{1}{\bar{\beta}_1}\left[\delta_{11} - \delta_{12} - \frac{2\pi\Phi_{e10}}{\Phi_0} - \kappa_{12}\left(\delta_{21} - \delta_{22} - \frac{2\pi\Phi_{e20}}{\Phi_0}\right)\right] - \sin\delta_{11}$$

$$\frac{\tau_1}{I_{01}}\dot{\delta}_{12} = J_1 + \frac{1}{\bar{\beta}_1}\left[\delta_{11} - \delta_{12} - \frac{2\pi\Phi_{e10}}{\Phi_0} - \kappa_{12}\left(\delta_{21} - \delta_{22} - \frac{2\pi\Phi_{e20}}{\Phi_0}\right)\right] - \sin\delta_{12}$$

$$\frac{\tau_2}{I_{02}}\dot{\delta}_{21} = J_2 - \frac{1}{\bar{\beta}_2}\left[\delta_{21} - \delta_{22} - \frac{2\pi\Phi_{e20}}{\Phi_0} - \kappa_{21}\left(\delta_{11} - \delta_{12} - \frac{2\pi\Phi_{e10}}{\Phi_0}\right)\right] - \sin\delta_{21}$$

$$\frac{\tau_2}{I_{02}}\dot{\delta}_{22} = J_2 + \frac{1}{\bar{\beta}_2}\left[\delta_{21} - \delta_{22} - \frac{2\pi\Phi_{e20}}{\Phi_0} - \kappa_{21}\left(\delta_{11} - \delta_{12} - \frac{2\pi\Phi_{e10}}{\Phi_0}\right)\right] - \sin\delta_{22}, \quad (14)$$

where $\kappa_{12} \equiv \kappa\sqrt{L_1/L_2}, \kappa_{21} \equiv \kappa\sqrt{L_2/L_1}$, and $\bar{\beta}_i \equiv \beta_i(1-\kappa^2)$, with $\kappa \equiv M/\sqrt{L_1 L_2}$. Note that κ can range from zero to one.

Before introducing signal and noise terms, we note a special case. If the SQUIDs are *identical* and *identically biased* ($J_1 = J_2 = J$, $\Phi_{e10} = \Phi_{e20} = \Phi_{e0}$), the dynamics above reduce to the much simpler single SQUID equations of motion (5) with a new effective nonlinearity parameter $\tilde{\beta} \equiv \beta(1+\kappa)$. Rescaling time by $\frac{\tau}{I_0}$ gives

$$\dot{\delta}_j = J + \frac{(-1)^j}{\tilde{\beta}}\left(\delta_1 - \delta_2 - \frac{2\pi\Phi_{e0}}{\Phi_0}\right) - \sin\delta_j \quad (j = 1, 2), \quad (15)$$

which may be treated as described in the preceding section and our recent work [9]. In the absence of noise, the loop fluxes evolve identically, with the system (15) describing the evolution of each SQUID. The question of phase locking in a similar multi-junction, two loop system was studied in [14]. Note that the general case of n globally coupled, identical, and identically biased SQUIDs may be characterized rather elegantly after iterative calculations starting with (11); for this case, we are able to write the dynamics, in the absence of noise terms, in closed form analogous to (14), whence we find that the dynamics collapses onto the description of a single SQUID with a "dressed" β as in (15):

$$\dot{\delta}_j = J + \frac{1-\kappa}{1 + (n-2)\kappa - (n-1)\kappa^2}\frac{(-1)^j}{\beta}\left(\delta_1 - \delta_2 - \frac{2\pi\Phi_{e0}}{\Phi_0}\right) - \sin\delta_j \quad (j = 1, 2), \quad (16)$$

$\kappa = M/L$, from which we recover (15) for $n = 2$.

We now consider the interesting situation of n identical and identically biased SQUIDs subject to different (internal) noise sources. The equations for the phase angles may be obtained directly from (11) by adding a (thermal) noise term, assumed to be Gaussian white noise $F_{kj}(t)$ ($k = 1, \ldots, n$; $j = 1, 2$), to each equation to model thermal noise arising in the Josephson junctions. The noise sources are assumed uncorrelated, and each source has autocorrelation $\langle F_{kj}(t)F_{kj}(t+s)\rangle = D_{kj}\delta(s)$. Note that even with identical and identically biased SQUIDs, we cannot collapse the dynamics onto two equations as in (16) because of the noise terms. In the absence of noise, however, the description (16) may be used to determine the

critical bias conditions for the onset of the oscillatory solutions, as in the preceding section.

We can compare several interesting cases: a single SQUID ($n = 1$), an array of uncoupled SQUIDs ($n > 1$, $\kappa = 0$), and an array of coupled SQUIDs ($n > 1$, $\kappa > 0$). Note that if we take as the array's output the circulating current in one member of the array, for $\kappa = 0$ we will clearly obtain the same results for $n = 1$ and $n > 1$; however, if we take as the output the sum of the circulating currents of all of the array elements, these two cases become distinct.

We simulated the above cases using $\beta = 2$ and an externally applied flux consisting of a dc bias and a sinusoidal target signal: $\Phi_{e0} = \Phi_{ex} + A\sin(\omega t)$ $(k = 1, \ldots, n)$. We bias the single SQUID such that the TC looks approximately like that in Fig. 1(a), panel $J = 0.1$, having a steep region around $\Phi_{ex} = 0.5$. To effect this biasing for our $\beta = 2$ SQUID, we set the bias current to $J = 0.40731$, giving a critical flux for the onset of running states of $\Phi_{ex1} = 0.495$ and producing a very steep region in the TC from about $\Phi_{ex1} = 0.495$ to about $\Phi_{ex2} = 0.505$. The *gain* (slope of the TC) at $\Phi_{ex} = 0.5$ in the absence of noise is approximately 53.1. We then set the bias current J of the coupled array such that the predicted gain (in the absence of noise) equals the gain of the single SQUID. For example, for $\kappa = 0.1$, the bias current needed to yield a gain of 53.1 in a four SQUID array is $J = 0.4777$. Note that (in the absence of noise) we can reduce the problem of predicting the gain of the array to one of predicting the gain of a single SQUID, using the fact that we can reduce the n coupled SQUIDs to a single one with a "dressed" β.

The circulating current's oscillation frequency is an important time scale to consider when performing simulations. The step size of the numerical integration should be much smaller than the period of this oscillation. As mentioned in the previous section, the circulating current's oscillation frequency is typically very high, and the electronics is only able to read out the time-averaged value of the circulating current. In the simulations, we effectively perform this averaging by looking only at frequencies in the power spectrum close to the target signal, which we set at a value much less that the circulating current's oscillation frequency.

Since we have chosen the bias currents to yield equal gains in the single SQUID and the array, we expect to get the same signal power out of both, at least in the limit of weak signal and noise. Concerning the noise, note that each SQUID in the array is subject to the same input signal, but each Josephson junction gives rise to its own thermal noise, uncorrelated with the other noise sources. Thus, coupling the SQUIDs or summing their outputs will give rise to an "averaging" over these uncorrelated noise sources. This should result in an increased SNR.

Let's consider the case of summing in more detail. All n of the SQUIDs are subjected to the same target signal, so their responses at the target signal will all be correlated with each other. If they are perfectly correlated, the amplitude of the summed output will be n times greater than a single output, and the summed signal power will be n^2 times greater. In contrast, the noise generated in the SQUIDs will be uncorrelated from SQUID to SQUID. The powers (rather than the amplitudes) of random, uncorrelated noises add, so the summed noise power will be only n

times greater than that at a single output. Hence, in the ideal case of perfectly correlated signals and uncorrelated noises, summing boosts the SNR by a factor of $n^2/n = n$ compared to the SNR of an individual output.

In practice, the summed output could be measured in a variety of ways. We could individually measure the shielding flux of each SQUID, or we could use a network of pickup coils connected in parallel to sense and sum the shielding fluxes of all of the SQUIDs.

Certainly the network of pickup coils would be much simpler to implement than measuring each SQUID individually. A further advantage of measuring the summed output (rather than measuring the individual outputs and then summing the measurements) would be that summing would also boost the signal power into the measurement device, and if the noise floor of the measurement device is the limiting factor in output SNR, this will increase the output SNR.

Of course, the summing network will also unavoidably cause a coupling between the SQUIDs. In fact, this sort of coupling is identical to the global coupling case we have been considering. Each SQUID feels a flux due to all the other SQUIDs (but not from itself, of course). But how would this coupling affect the SNR improvement produced by summing? By causing more correlation between the SQUIDs, strong coupling could conceivably kill the improvement. Our simulations address this question for an array of four SQUIDs.

By summing the circulating currents of 4 uncoupled SQUIDs, we get a 6 dB improvement over a single SQUID. This is what one would predict from theory: by summing 4 uncoupled SQUIDs one gets $4^2 = 16$ times the signal power (12 dB increase) and just 4 times the noise power (6 dB increase) of a single SQUID, yielding 4 times the SNR (6 dB improvement). Figure 2 illustrates this result for a target signal amplitude of $A = 0.000125893$ and frequency $\omega = \pi/1000$ [using the rescaled time units of equation (16)]. In the output SNR plot, the uncoupled array ($\kappa = 0$) "summed output" scenario consistently exceeds the output SNR of a single uncoupled SQUID by approximately 6 dB, over the range of Josephson junction noise strengths plotted. The output signal power plot shows the uncoupled array "summed output" scenario exceeding the output signal power of a single uncoupled SQUID by approximately 12 dB.

When we simulate a system with moderate coupling ($\kappa = 0.1$) between elements, we find nearly the SNR obtained by summing the outputs of uncoupled elements. Referring again to Fig. 2, we find an approximately 4.6 dB SNR improvement with summing and coupling, while coupling boosts the SNR of an individual array element by about 2.3 dB. For low noise strengths, the coupled array summed output signal power matches that of the uncoupled array, but for higher noise the effect of coupling is to reduce the power somewhat.

In this system, summing *and* coupling does not seem to beat summing alone. However, the important observation is that moderate coupling does not seriously hurt the summing effect. This means that in practice the simple summing network described above can be used, and the side effect of coupling will not kill the SNR-improving effect of summing.

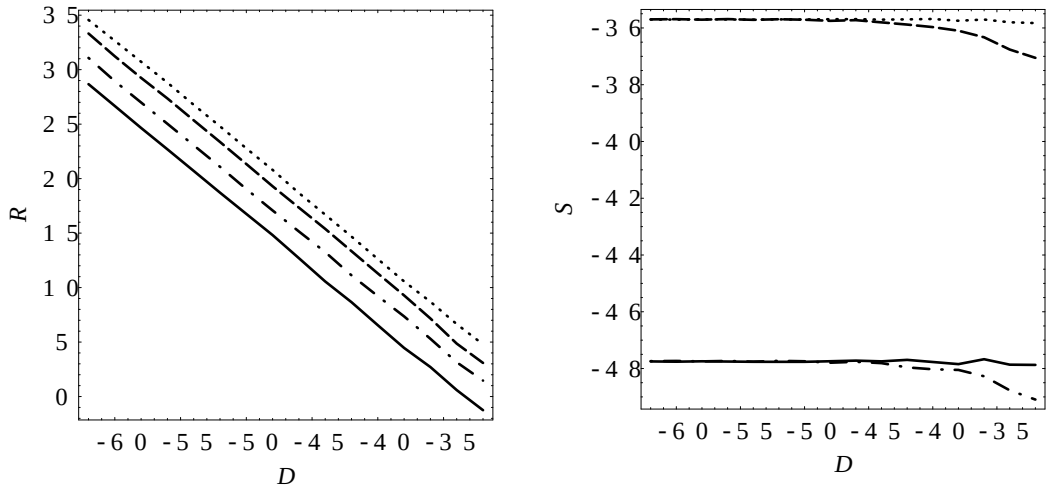

FIGURE 2. Output SNR R and output signal power S. Solid line: $\kappa = 0$, single output. Dot-dashed line: $\kappa = 0.1$, single output. Dashed line: $\kappa = 0.1$, summed output. Dotted line: $\kappa = 0$, summed output. All scales are in decibels, i.e. $10 \log_{10}(\cdot)$.

The results shown in Fig. 2 are for a "weak" signal, meaning that $A \ll (\Phi_{ex2} - \Phi_{ex1})/2$. Thus, the response to the target signal is nearly linear provided the noise is also weak. We have obtained qualitatively similar results for strong signals having $A \lesssim (\Phi_{ex2} - \Phi_{ex1})/2$, but in this case the response nonlinearity causes the output signal power (summed or not) to be slightly higher with $\kappa = 0.1$ than with $\kappa = 0$, provided the noise is weak. As the noise level is increased, the fact mentioned above concerning a slight coupling-related power reduction at higher noises causes the curves for $\kappa = 0.1$ and $\kappa = 0$ to cross, with the coupled case falling below the uncoupled case.

In simulations with $\kappa = 0.5$ (not shown), we find that the strong coupling *greatly* reduces the SNR-improving effect. We may therefore draw another important conclusion: there is evidently an *optimal* value of κ. If κ is too large, the summing effect does not work. If κ is too small, very little signal will be coupled into the summing network, and the summed signal will fall below the noise floor of the measurement system.

ACKNOWLEDGMENTS

We gratefully acknowledge support from the Office of Naval Research, as well as the Internal Research program at SPAWAR Systems Center, San Diego. We also acknowledge the Department of Defense High Performance Computing Modernization Program for a CHSSI Computation Electronics and Nanoelectronics grant and computer time allocations on the NAVO and ERDC SGI/Cray T3E supercomputers.

REFERENCES

* Electronic address: inchiosa@nosc.mil, web site: http://hpcweb.nosc.mil/sr/
† Electronic address: bulsara@nosc.mil

1. A. Barone, G. Paterno; *Physics and Applications of the Josephson Effect*, (J. Wiley, NY 1982)
2. For good overviews see K. Wiesenfeld, F. Moss; Nature **373**, 33 (1995). A. Bulsara, L. Gammaitoni; Phys. Today **49**, 39 (1996). L. Gammaitoni, P. Hanggi, P. Jung, F. Marchesoni; Rev. Mod. Phys. **70**, 223 (1998).
3. A. Hibbs, A. Singsaas, E. Jacobs, A. Bulsara, J. Bekkedahl, F. Moss; J. Appl. Phys. **77**, 2582 (1995). R. Rouse, S. Han, J. Lukens; Appl. Phys. Lett. **66**, 108 (1995).
4. A. Bulsara, M. Inchiosa, L. Gammaitoni; Phys. Rev. Lett. **77**, 2162 (1996); M. Inchiosa, A. Bulsara, L. Gammaitoni; Phys. Rev. **E55**, 4049 (1997). M. E. Inchiosa, A. R. Bulsara; Phys. Rev. **E58**, 115 (1998).
5. See e.g. C. Gardiner; *Handbook of Stochastic Methods*, (Springer Verlag, Berlin 1983).
6. M. E. Inchiosa, A. R. Bulsara, A. D. Hibbs, B. Whitecotton; Phys. Rev. Lett. **80**, 1381 (1998).
7. J. Robinson, D. Asraf, A. Bulsara, M. Inchiosa; Phys. Rev. Lett. **81**, 2850 (1998).
8. A. Hibbs, B. Whitecotton; in *Applied Nonlinear Dynamics and Stochastic Systems Near the Millenium*, eds. J. Kadtke, A. Bulsara (AIP, New York 1997).
9. M. Inchiosa, A. Bulsara, K. Wiesenfeld, L. Gammaitoni; Phys. Lett. **A252**, 20 (1999).
10. A. de Waele, R. de Bruyn Ouboter; Physica **41**, 225 (1969). A. Matsinger, R. de Bruyn Ouboter, H. van Beelen; Physica **94B**, 91 (1978). C. Tesche; J. Low Temp. Phys. **44**, 119 (1981). E. Ben-Jacob, D. Bergman, Y. Imry, B. Matkowsky, Z. Schuss; J. Appl. Phys. **54**, 6533 (1983). T. Ryhanen, H. Seppa, R. Ilmoniemi, J. Knuutila; J. Low Temp. Phys. **76**, 287 (1989).
11. See e.g. N. Minorsky; *Nonlinear Oscillations* (Kreiger, N.Y. 1987).
12. E. Ben-Jacob, Y. Imry; J. Appl. Phys. **52**, 6806 (1981). P. Carelli, G. Paterno; in *Principles and Applications of Superconducting Quantum Interference Devices*, ed. A. Barone (World Scientific, Singapore 1992).
13. See e.g. M. Locher, D. Cigna, E. Hunt, G. Johnson, F. Marchesoni, L. Gammaitoni, M. Inchiosa, A. Bulsara; Chaos **8**, 604 (1998), and references therein.
14. A. N. Grib, P. Seidel, M. Darula; J. Low Temp. Phys. **112**, 323 (1998).